ChemistryOPEN Full Papers

ChemPubSoc Europe

Open Access

DOI: 10.1002/open.201402027

Inhibition of Insulin-Regulated Aminopeptidase (IRAP) by Arylsulfonamides

Sanjay R. Borhade,[b] Ulrika Rosenström,[b] Jonas Sävmarker,[c] Thomas Lundbäck,[d] Annika Jenmalm-Jensen,[d] Kristmundur Sigmundsson,[d] Hanna Axelsson,[d] Fredrik Svensson,[b] Vivek Konda,[b] Christian Sköld,[b] Mats Larhed,[e] and Mathias Hallberg*[a]

The inhibition of insulin-regulated aminopeptidase (IRAP, EC 3.4.11.3) by angiotenesin IV is known to improve memory and learning in rats. Screening 10 500 low-molecular-weight compounds in an enzyme inhibition assay with IRAP from Chinese Hamster Ovary (CHO) cells provided an arylsulfonamide (*N*-(3-(1*H*-tetrazol-5-yl)phenyl)-4-bromo-5-chlorothiophene-2-sulfonamide), comprising a tetrazole in the *meta* position of the aromatic ring, as a hit. Analogues of this hit were synthesized, and their inhibitory capacities were determined. A small structure–activity relationship study revealed that the sulfonamide function and the tetrazole ring are crucial for IRAP inhibition. The inhibitors exhibited a moderate inhibitory potency with an $IC_{50} = 1.1 \pm 0.5$ μM for the best inhibitor in the series. Further optimization of this new class of IRAP inhibitors is required to make them attractive as research tools and as potential cognitive enhancers.

Introduction

It was reported 25 years ago that intracerebroventricular (i.c.v.) injection of angiotensin IV (Ang IV, Val-Tyr-Ile-His-Pro-Phe), an angiotensin II metabolite, improved memory and learning in rats.[1] The positive impact of Ang IV on cognition was subsequently confirmed in a series of animal models in both rats and mice.[2–5] Structurally related analogues to Ang IV, such as the endogenous LVV-hemorphin-7 (Leu-Val-Val-Tyr-Pro-Trp-Thr-Glu-Arg-Phe), in which a tyrosine residue is attached to lipophilic amino acid residues, as in Ang IV, exhibited similar outcomes.[6] These abilities to improve processes related to memory and learning have attracted considerable interest in recent years.[7,8]

A specific binding site for Ang IV was identified in 1992,[9,10] and high densities of the binding sites were found in areas of the brain that are associated with cognitive, sensory, and motor functions, including the hippocampus.[9] Insulin-regulated aminopeptidase (IRAP), a high-affinity receptor for Ang IV, was purified in 2001.[11] IRAP has been identified as cystinyl aminopeptidase (CAP, EC 3.4.11.3), placental leucine aminopeptidase (P-LAP, soluble human homologue), oxytocinase, gp160, or vp165.[12–14] IRAP, a single-spanning transmembrane zinc-metallopeptidase that belongs to the M1 family of aminopeptidases,[15] has attracted awareness as a potential target for pharmaceuticals aimed at the treatment of cognitive disorders.[8,16–18] It is hypothesized that the inhibition of the catalytic activity of IRAP by the hexapeptide Ang IV results in longer half-lives of endogenous substrates to IRAP, such as vasopressin and oxytocin, which are macrocyclic disulfides and are known to exert favorable influences on cognitive parameters in the brain,[19] although several alternative and relevant hypotheses explaining the action of Ang IV have been proposed.[20,21]

We recently reported the syntheses and IRAP inhibition data from a series of constrained macrocycles derived from Ang IV and with structural similarities to, for example, oxytocin in the N terminus.[22–24] Among those, HA-08 (**1**), which has a β3hTyr residue in a 13-membered macrocyclic system is 20 times more potent than Ang IV as an IRAP inhibitor.[24] Although further optimization and application of the metathesis reaction delivered very potent and more metabolically stable macrocyclic carba analogues,[22] these inhibitors, designed from structures of cyclic substrates, are still too peptidic and not likely to be able to enter the brain.

[a] *Dr. M. Hallberg*
Beijer Laboratory, Department of Pharmaceutical Biosciences
Division of Biological Research on Drug Dependence
BMC, Uppsala University, P.O. Box 591, 751 24 Uppsala (Sweden)
E-mail: mathias.hallberg@farmbio.uu.se

[b] *Dr. S. R. Borhade, Dr. U. Rosenström, F. Svensson, Dr. V. Konda, Dr. C. Sköld*
Organic Pharmaceutical Chemistry, Department of Medicinal Chemistry
BMC, Uppsala University, P.O. Box 574, 751 23 Uppsala (Sweden)

[c] *Dr. J. Sävmarker*
Beijer Laboratory, Department of Medicinal Chemistry
BMC, Uppsala University, P.O. Box 574, 751 23 Uppsala (Sweden)

[d] *Dr. T. Lundbäck, Dr. A. Jenmalm-Jensen, Dr. K. Sigmundsson, H. Axelsson*
Chemical Biology Consortium Sweden, Science for Life Laboratory
Division of Translational Medicine and Chemical Biology
Department of Medical Biochemistry and Biophysics
Karolinska Institutet, Stockholm 171 77 (Sweden)

[e] *Prof. M. Larhed*
Department of Medicinal Chemistry, Science for Life Laboratory
BMC, Uppsala University, P.O. Box 574, 751 23 Uppsala (Sweden)

Supporting information for this article is available on the WWW under http://dx.doi.org/10.1002/open.201402027.

Recently, Albiston et al. discovered a series of drug-like IRAP inhibitors encompassing a benzopyran system.[7,25,26] These inhibitors were identified after in silico screening of 1.5 million commercially available compounds against an IRAP model structure. After i.c.v. administration of one of these inhibitors, HFI-419 (**2**), a pronounced enhancement of memory in two memory paradigms in rat was observed. We were encouraged by these findings and performed a screening campaign of a library of 10500 low-molecular-weight compounds and measured the inhibition of the catalytic activity of IRAP from Chinese Hamster Ovary (CHO) cells. After subsequent hit confirmation experiments, we identified sulfonamide **3** as one of the most promising compounds. We herein report the syntheses of a series of analogues of **3**, their inhibitory capacity, and structure–activity relationships of this new class of IRAP inhibitors.

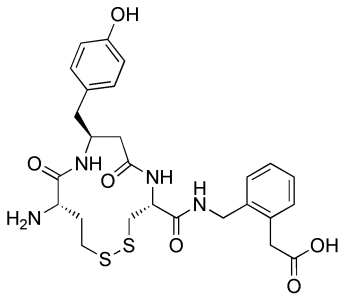

HA-08 (**1**)

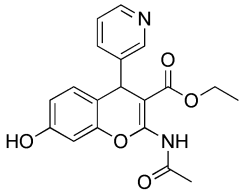

HFI-419 (**2**)

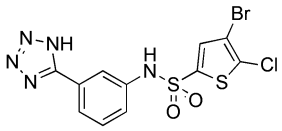

3

Results and Discussion

In the primary high-throughput screen (HTS), analogues of **3**, with a carboxylate group rather than the bioisosteric tetrazole in the *ortho*, *meta*, or *para* positions of the aromatic ring, were all found to be devoid of capacity to inhibit or be very weak inhibitors of IRAP, suggesting that an acidic function is not a sufficient criterion to achieve inhibition. Hence, the IC_{50} values for the *meta* carboxylate and the corresponding ethyl ester were determined to be greater than 125 μM in the hit confirmation experiments. Furthermore, the regioisomer of **3**, with the tetrazole ring positioned in the *para* position rather than in the *meta* position, was inactive according to the preliminary data.

To examine the basic structure–activity relationships, compounds **3**, **7**–**22**, **25**, and **27** were synthesized and evaluated as inhibitors in an IRAP enzyme assay with a special emphasis to assess whether the thiophene ring, sulfonamide function, and the acidic NH of the tetrazole are prerequisites for binding to IRAP.

The target compounds **3**, **7**–**22**, **25**, and **27** were synthesized as shown in Schemes 1–3. Compound **3**, **7**–**22** were synthesized from 3-amino phenyltetrazole (**4**) or 3-amino-*N*-methylbenzamide (**5**) reacting with the corresponding aryl/heteroaryl sulfonyl chloride to give good to excellent yields.[27] N-Methylated arylsulfonamide **25** was synthesized from 3-amino benzonitrile (**23**) as shown in Scheme 2. First, the sulfonylation of 4-bromo-5-chlorothiophene-2-sulfonyl chloride with **23** gave the desired product, 4-bromo-5-chloro-*N*-(3-cyanophenyl)thiophene-2-sulfonamide, which was used without purification for further treatment with methyl iodide in presence of sodium hydride to afford compound **24** in 78% overall yield. The tetrazole ring formation starting from cyanophenyl sulfonamide (**24**) was successfully achieved via the reported method of Koguro et al.[28] by using sodium azide and triethylammonium hydrochloride salt in dry toluene to deliver product **25** in 71% yield. For the synthesis of compound **27**, 4-bromo-5-chlorothiophene-2-carboxylic acid was coupled with 3-amino phenyltetrazole via standard peptide coupling conditions using benzotriazol-1-yl-oxytripyrrolidinophosphonium hexafluorophosphate (PyBOP) as a peptide coupling reagent for 18 hours at 25 °C with dimethylformamide (DMF) as the solvent (Scheme 3).[29]

The biological data from the evaluation of **3**, **7**–**22**, **25**, and **27** as inhibitors of IRAP are presented in Table 1. The NH group on the tetrazole ring seems essential to the inhibitory activity since methylation of the nitrogen affords inactive compound **7**. To find out whether a considerably less acidic NH is sufficient for activity, compound **8** was evaluated and found to be inactive as well. Apparently a tetrazole with an acidic hydro-

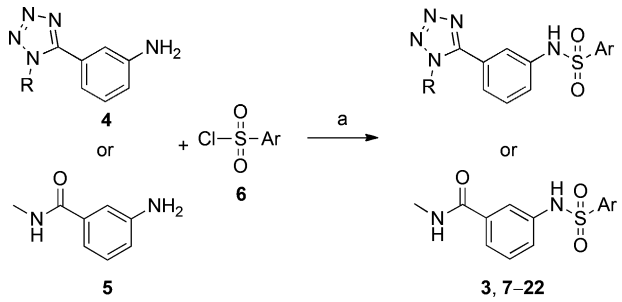

Scheme 1. Synthesis of IRAP inhibitors **3**, **7**–**22**. *Reagents and conditions*: a) CH_2Cl_2, pyridine, 25 °C, 14 h.

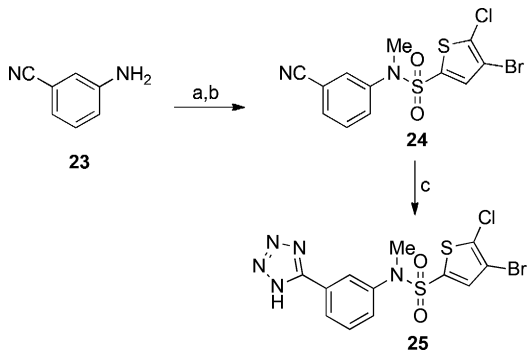

Scheme 2. Synthesis of IRAP inhibitor **25**. *Reagents and conditions*: a) 4-bromo-5-chlorothiophene-2-sulfonyl chloride, CH_2Cl_2, pyridine, 25 °C, 14 h; b) THF, NaH, MeI, 0 °C to 25 °C, 3 h, 78%; c) NaN_3, $Et_3N{\cdot}HCl$, toluene reflux, 12 h, 71%.

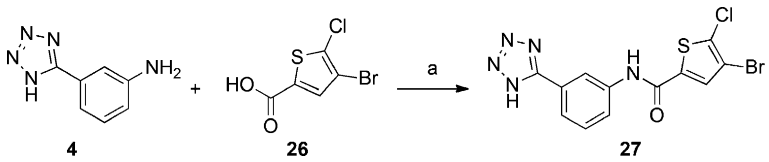

Scheme 3. Synthesis of IRAP inhibitors **27**. *Reagents and conditions*: a) DMF, PyBOP, Et_3N, 25 °C, 18 h, 81 %.

gen but neither a carboxylate nor amide in the *meta* position of the aromatic ring results in IRAP inhibitory activity.

Classic bacteriostatic arylsulfonamides, such as sulfamethoxazole and sulfadiazine, which are structurally similar to **3**, are weak acids. The presence of the moderately acidic NH is important to retain activity since methylation, leading to **25**, rendered a considerably less potent inhibitor. Furthermore, displacement of the sulfonamide linker for an amide provided the

Table 1. Biological evaluation of compounds **3**, **7**–**22**, **25**, and **27** in the IRAP inhibition assay.

Compd	Structure	IC_{50} [μM][a]	Compd	Structure	IC_{50} [μM][a]
3	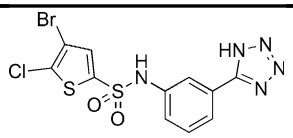	2.1 ± 1.2 (15)	**16**	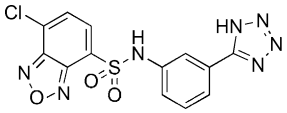	1.3 ± 0.75 (3)
7	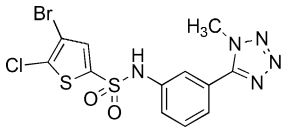	> 125[b] (3)	**17**	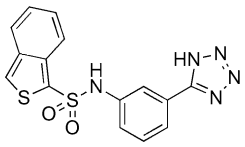	39 ± 3.4[b] (2)
8	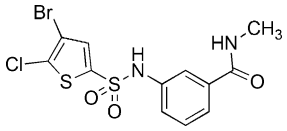	> 125[b] (3)	**18**	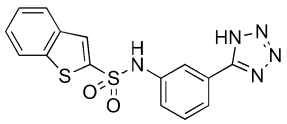	16 ± 4.9 (2)
9	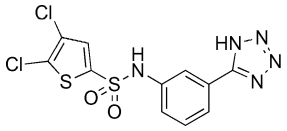	1.8 ± 1.3 (4)	**19**	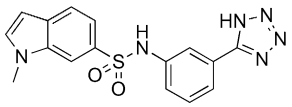	22 ± 6.4 (2)
10	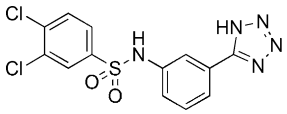	1.1 ± 0.46 (4)	**20**	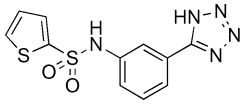	> 125[b] (2)
11	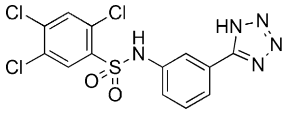	2.9 ± 0.28 (3)	**21**	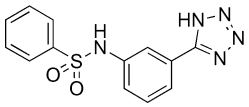	> 125[b] (2)
12	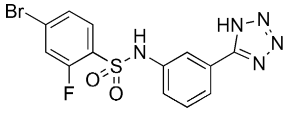	1.6 ± 0.93 (3)	**22**	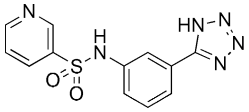	> 125[b] (2)
13	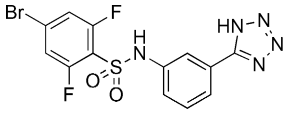	7.9 ± 2.1 (2)	**25**	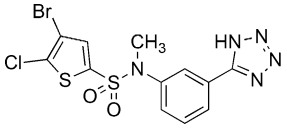	58 ± 23[b] (3)
14	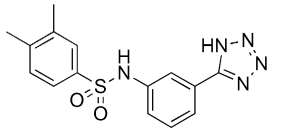	3.1 ± 1.8 (3)	**27**	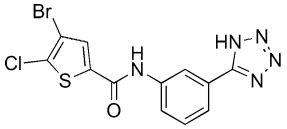	67 ± 7.8[b] (3)
15	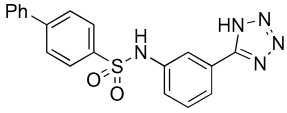	44 ± 3.3[b] (3)			

[a] IC_{50} is defined as the compound concentration required to inhibit IRAP activity by 50 %. Values represent the mean ± standard deviation of best-fit values from individual test occasions (carried out on different days). The number of separate test occasions is given in parentheses. [b] Fitting was performed with maximal inhibition fixed to 100 %. No values above 125 μM are reported as this was the highest compound concentration tested.

weak inhibitor **27**. The loss of most of the inhibitory potency of **27** could be attributed to 1) the restricted rotation of the amide bond not allowing adoption of an optimal binding to IRAP, 2) the loss of an acidic NH, or alternatively 3) the sulfonamide oxygen(s) being crucial for binding. Substitution of the 4-bromo for a 4-chloro group to provide **9** did not result in an improvement in the inhibitory activity, but substitution of the thiophene for a benzene ring resulted in a small improvement (c.f., compounds **9** and **10**). Furthermore, an additional chloro substituent in the *ortho* position rendered an inhibitor with a good inhibitory capacity (**11**). A fluoro group in the *ortho* position of a *para* bromo derivative (**12**) provided a potent inhibitor while with two *ortho* substituents, as in compound **13**, a decline in potency was observed. Compound **14** with two methyl groups located in the *meta* and *para* positions exhibited good potency, but biphenyl compound **15** was found to be more than ten times less active ($IC_{50} = 3.1 \pm 1.8$ vs 44 ± 3.3 μM). The observation that a chloro or fluoro substituent was accepted in the *ortho* position by the enzyme prompted us to make the more bulky annelated benzooxadiazole derivative (**16**), which acted as a potent IRAP inhibitor. Benzothiophenes **17** and **18** and methylindole derivative **19** were approximately 10 times less active as inhibitors.

It is notable that the nonsubstituted thiophene, benzene, and pyridine derivatives **20**, **21**, and **22**, respectively, exhibited all very poor abilities to inhibit the protease. Furthermore, IRAP inhibitors **10**, **14**, and **16** exhibited a more than 10-fold preference for IRAP than for the protein homologue aminopeptidase N (APN) (unpublished data).

In an attempt to rationalize the observed activities of the synthesized compounds, a docking study of the series was conducted using Glide (version 5.8; for details, see Experimental Section). To date, no crystal structure of IRAP has been reported. In order to model the binding of the inhibitors, we utilized APN for which several high-resolution protein–ligand co-crystal structures have been reported.[30] Twelve of the sixteen amino acids that are found in the catalytic site of APN are conserved in IRAP, where the catalytic site is defined as within 3 Å of Val and Tyr in Ang IV when co-crystallized in APN (PDB code 4FYS[30]); see Supporting Information for sequence alignment. Since APN and IRAP have a high sequence identity in proximity to the catalytic zinc, where we hypothesize that the modeled ligands are binding, we find it reasonable to assume that models of the binding modes found in the catalytic region of APN can be extended to IRAP.

The docking produced several possible binding modes but all with rather poor Glide docking scores. However, by visual inspection, we identified a potential binding mode of the series that to some extent accounts for the observed structure–activity relationships. Figure 1 shows this binding mode illustrated using compound **3**. In the proposed binding mode, the negatively charged tetrazole of **3** is involved in zinc binding and, in addition, is stabilized in the catalytic site by a hydrogen bond to Tyr477 (IRAP: Tyr549). This Tyr residue is highly conserved in the M1 family of metalloproteases and is indicated to be important for binding and stabilization of the catalytic transition state.[30] Furthermore, the compound is stacked between Phe472 (IRAP: Phe544) and Phe896 (IRAP: Tyr961) in the active site. The stacking interaction with Phe544 in IRAP has previously been reported as a key interaction for ligand and substrate binding.[31,32] Two of the amino acids in contact with compound **3** differ between APN and IRAP. Phe896 is replaced by Tyr in IRAP, and Gln213 is replaced by Glu. We anticipate that the difference between the protein structures should not have a significant impact on the present binding mode model of **3** as the aromatic stacking interaction should remain largely the same changing from Phe to Tyr and since Gln213 is not involved in any specific interaction with the ligand.

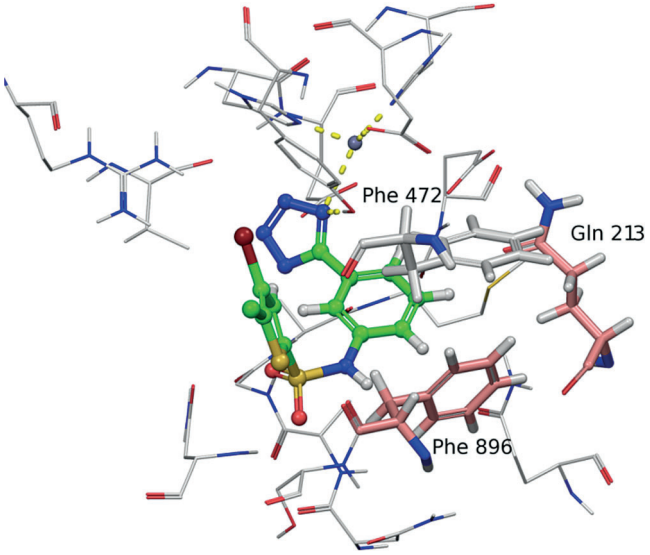

Figure 1. Potential binding mode of **3** shown in the homologue aminopeptidase N (APN) active site (PDB code 4FYS[30]). The catalytic zinc is depicted as a grey bullet, and amino acids discussed in the text are highlighted; Gln213 and Phe896 are displayed in pink sticks, and Phe472 is displayed in light grey sticks.

This binding mode model fits nicely with the inactivity of the methylated tetrazole found in **7**, which cannot produce a complimentary negative charge to the catalytic zinc. The model can possibly also account for the preference for tetrazole over carboxylic acid by the different directionality of their zinc binding moiety. Replacing the tetrazole with a carboxylic acid, the carboxylate interacts with the catalytic zinc in the least common *anti* interaction.[33] Furthermore, N-methylation of the sulfonamide in **25** would, in this binding mode, generate a steric clash with the enzyme, thus possibly explaining the decrease in activity caused by this structural modification. However, the decreased activity of compounds extended in the phenyl *para* position is not accounted for properly by this model. In order to fully conclude the binding mode of this series of compounds, more experimental information needs to be obtained. It is possible that a crystal structure of IRAP would reveal differences in structure that are hard to predict using the approach applied herein, and thus fully account for the observed structure–activity relationships.

Conclusions

New improved enhancers of cognitive functions are persistently desired for the treatment of the cognitive decline associated with Alzheimer's disease, brain trauma, and cerebral ischemia, since the clinical studies of the cholinesterase inhibitors and *N*-methyl-D-aspartate (NMDA) receptor antagonists used today have been mostly disappointing.[34,35] It is therefore not surprising that the receptor(s) involved in the beneficial effects of Ang IV has emerged as a relevant new target for drug intervention. High-throughput screening of 10500 low-molecular-weight compounds resulted in a series of hits, one of which was sulfonamide **3**. As deduced from an analysis of analogues to **3**, for example the corresponding carboxylic acid that was assayed in the primary screen and found to be inactive, and from a small structure–activity relationship study involving compounds **3**, **7**–**22**, **25**, and **27**, it is concluded that the sulfonamide function and a tetrazole ring in the *meta* position of the aromatic ring are crucial for IRAP inhibition. Further optimization, together with characterization of their mechanism of action and modes of binding are required to make these compounds attractive as research tools for in vivo studies and as potential cognitive enhancers.

Experimental Section

Chemistry

General information and materials: All chemicals were purchased from Sigma–Aldrich/Apollo scientific/Acros and used as received. Purification was performed on column chromatography using silica gel (60–120 mesh size) and then preparative thin-layer chromatography (TLC) or preparative reversed-phase high-performance liquid chromatography (RP-HPLC) (UV-triggered (254 nm) fraction collection with a Dionex UltiMate 3000 HPLC system, using an Agilent PrepHT Zorbax SB-C8 column (21.2×150 mm, 5 μm particle size) or a Macherey–Nagel Nucleodur C18 column (21×125 mm, 5 μm particle size), and H_2O/CH_3CN/0.05% HCOOH as eluents in a gradient (30–90%, 10 mL min^{-1} over 10 min). Analytical HPLC-mass spectrometry (HPLC-MS) was performed on a Dionex UltiMate 3000 HPLC system with a Bruker amaZon SL ion trap mass spectrometer and detection by UV (diode array detector) and MS (electrospray ionization, ESI− or ESI+), using a Phenomenex Kinetex C18 column (50×3.0 mm, 2.6 μm particle size, 100 Å pore size) and a flow rate of 1.5 mL min^{-1}. A gradient of H_2O/CH_3CN/0.05% HCOOH was used. Melting points were determined on an electrothermal melting point apparatus and are uncorrected. Infrared (IR) spectra were obtained on a Varian 1000 FT-IR spectrometer; absorbances are reported in cm^{-1}. ^{1}H and ^{13}C NMR spectra were obtained on a Varian Mercury spectrometer (^{1}H: 400 MHz, ^{13}C: 101 MHz) using $CDCl_3$, CD_3OD, [D_6]acetone, or [D_6]DMSO as the solvent. High-resolution mass spectra (HRMS) were recorded on a Micromass Q-Tof2 mass spectrometer equipped with an electrospray ion source. Compounds **11**, **12**, **14**, **16**, and **18** are previously reported.[27]

General procedure for the synthesis of 3, 7–22: To a solution of appropriate amine (**4** or **5**) (1.0 mmol) in anhydrous CH_2Cl_2 (5 mL), under an atmosphere of nitrogen, was added appropriate sulfonyl chloride (1.2 mmol) and pyridine (3.0 mmol). The resulting reaction mixture was stirred at RT overnight and then quenched with saturated aq NH_4Cl (20 mL); the pH was adjusted to around 4 by addition of 1 M aq HCl. The aqueous phase was extracted with CH_2Cl_2 (3×10 mL). The combined organic phase was dried over Na_2SO_4, filtered, and evaporated under reduced pressure. The residue obtained was purified by silica gel flash column chromatography (CH_2Cl_2/MeOH, 98:2→90:10) to give the corresponding product.

***N*-(3-(1*H*-Tetrazol-5-yl)phenyl)-4-bromo-5-chlorothiophene-2-sulfonamide (3)**: White solid (358 mg, 85%); mp: 211–213 °C; ^{1}H NMR (400 MHz, [D_6]DMSO): δ = 7.89 (t, J = 1.9 Hz, 1H), 7.83–7.75 (m, 1H), 7.69 (s, 1H), 7.56 (t, J = 8.0 Hz, 1H), 7.35 ppm (ddd, J = 8.2, 2.2, 1.0 Hz, 1H); ^{13}C NMR (101 MHz, [D_6]DMSO): δ = 155.93, 138.47, 138.11, 134.13, 132.85, 131.11, 126.18, 123.89, 123.47, 119.31, 112.03 ppm; HRMS (ESI+): m/z $[M+H]^+$ calcd for $C_{11}H_8BrClN_5O_2S$: 419.8991, found: 419.8981; IR (neat): $\tilde{\nu}$ = 3247, 1624, 1583, 1572, 1479, 1403, 1372, 1336, 1314, 1158, 1040, 1022, 935 cm^{-1}.

4-Bromo-5-chloro-*N*-(3-(1-methyl-1*H*-tetrazol-5-yl)phenyl)thiophene-2-sulfonamide (7): White solid (387 mg, 89%); mp: 89–91 °C; ^{1}H NMR (400 MHz, [D_6]DMSO): δ = 11.08 (s, 1H), 7.73 (s, 1H), 7.64 (dt, J = 6.7, 1.6 Hz, 2H), 7.61–7.55 (m, 1H), 7.43–7.39 (m, 1H), 4.13 ppm (s, 3H); ^{13}C NMR (101 MHz, [D_6]acetone): δ = 154.42, 139.22, 138.50, 134.76, 133.96, 131.31, 126.63, 126.51, 124.40, 122.20, 112.18, 35.64 ppm; HRMS (ESI+): m/z $[M+H]^+$ calcd for $C_{12}H_{10}BrClN_5O_2S_2$: 433.9148, found: 433.9150; IR (neat): $\tilde{\nu}$ = 3057, 1738, 1592, 1485, 1404, 1342, 1214, 1154, 1023, 941 cm^{-1}.

3-(4-Bromo-5-chlorothiophene-2-sulfonamido)-*N*-methylbenzamide (8): White solid (344 mg, 84%); mp: 195–197 °C; ^{1}H NMR (400 MHz, [D_6]acetone): δ = 7.86 (td, J = 1.8, 0.6 Hz, 1H), 7.81 (s, 1H), 7.67 (dt, J = 7.3, 1.5 Hz, 1H), 7.48 (s, 1H), 7.48–7.39 (m, 2H), 2.90 ppm (d, J = 4.6 Hz, 3H); ^{13}C NMR (101 MHz, [D_6]acetone): δ = 167.13, 139.58, 138.20, 137.20, 134.41, 133.59, 130.28, 124.64, 124.48, 121.59, 112.00, 26.81 ppm; HRMS (ESI+): m/z $[M+H]^+$ calcd for $C_{12}H_9BrClN_2O_2S_2$: 408.9083, found: 408.9093; IR (neat): $\tilde{\nu}$ = 3424, 2929, 1739, 1641, 1550, 1472, 1401, 1336, 1220, 1147, 1009 cm^{-1}.

***N*-(3-(1*H*-Tetrazol-5-yl)phenyl)-4,5-dichlorothiophene-2-sulfonamide (9)**: White solid (312 mg, 89%); mp: 212–214 °C; ^{1}H NMR (400 MHz, [D_6]acetone): δ = 8.10 (ddd, J = 2.3, 1.6, 0.5 Hz, 1H), 7.95 (ddd, J = 7.7, 1.6, 1.1 Hz, 1H), 7.58 (t, J = 7.8 Hz, 1H), 7.55 (s, 1H), 7.50 ppm (ddd, J = 8.1, 2.3, 1.1 Hz, 1H); ^{13}C NMR (101 MHz, [D_6]acetone): δ = 157.54, 138.67, 138.04, 132.25, 131.80, 131.44, 127.40, 125.40, 124.89, 124.51, 120.55 ppm; HRMS (ESI+): m/z $[M+H]^+$ calcd for $C_{11}H_{10}Cl_2N_5O_2S_2$: 375.9496, found: 375.9498; IR (neat): $\tilde{\nu}$ = 3237, 1740, 1573, 1478, 1402, 1324, 1230, 1151, 1024, 933, 882 cm^{-1}.

***N*-(3-(1*H*-Tetrazol-5-yl)phenyl)-3,4-dichlorobenzenesulfonamide (10)**: White solid (300 mg, 81%); mp: 184–186 °C; ^{1}H NMR (400 MHz, [D_6]acetone): δ = 9.49 (s, 1H), 8.05 (ddd, J = 2.2, 1.7, 0.5 Hz, 1H), 7.98 (dd, J = 2.0, 0.5 Hz, 1H), 7.89 (ddd, J = 7.7, 1.6, 1.1 Hz, 1H), 7.82–7.72 (m, 2H), 7.52 (td, J = 7.9, 0.5 Hz, 1H), 7.43 ppm (ddd, J = 8.2, 2.3, 1.1 Hz, 1H); ^{13}C NMR (101 MHz, [D_6]acetone): δ = 157.48, 140.64, 139.09, 137.85, 133.77, 132.43, 131.36, 129.82, 127.82, 127.27, 124.44, 124.23, 120.22 ppm; HRMS (ESI+): m/z $[M+H]^+$ calcd for $C_{13}H_{10}Cl_2N_5O_2S$: 369.9932, found: 369.9930; IR (neat): $\tilde{\nu}$ = 3178, 1740, 1564, 1484, 1373, 1329, 1156, 1093, 1031, 949 cm^{-1}.

***N*-(3-(1*H*-Tetrazol-5-yl)phenyl)-2,4,5-trichlorobenzenesulfonamide (11)**: White solid (312 mg, 77%); mp: 250–254 °C; ^{1}H NMR (400 MHz, CD_3OD): δ = 10.08 (br s, 1H), 8.33 (m (s), 1H), 8.16 (m, 1H), 8.0 (m (s), 1H), 7.94 (m, 1H), 7.64–7.56 ppm (m, 2H); ^{13}C NMR (101 MHz, acetone): δ = 159.19, 137.79, 137.66, 136.87, 133.38,

132.93, 131.45, 130.75, 130.61, 123.51, 122.80, 118.84, 118.78 ppm; HRMS (ESI+): *m/z* $[M+MeCN+H]^+$ calcd for $C_{15}H_{12}Cl_3N_6O_2S$: 444.9808, found: 444.9832; IR (neat): $\tilde{\nu}$ = 3237, 3093, 2360, 1891, 1566, 1173, 930, 687 cm^{-1}.

***N*-(3-(1*H*-Tetrazol-5-yl)phenyl)-4-bromo-2-fluorobenzenesulfonamide (12)**: White solid (283 mg, 71%); mp: 196–198 °C; ^1H NMR (400 MHz, [D$_6$]acetone): δ = 8.07 (ddd, *J* = 2.2, 1.6, 0.6 Hz, 1H), 7.90–7.79 (m, 2H), 7.63 (dd, *J* = 9.7, 1.8 Hz, 1H), 7.57 (ddd, *J* = 8.4, 1.9, 0.8 Hz, 1H), 7.50 (ddd, *J* = 8.1, 7.4, 0.6 Hz, 1H), 7.45 ppm (ddd, *J* = 8.2, 2.2, 1.3 Hz, 1H); ^{13}C NMR (101 MHz, [D$_6$]acetone): δ = 160.63, 158.05, 138.89, 132.94, 131.27, 129.13, 129.09, 127.30, 124.23, 123.64, 121.74, 121.50, 119.67 ppm; HRMS (ESI+): *m/z* $[M+H]^+$ calcd for $C_{13}H_{10}BrFN_5O_2S$: 397.9723, found: 397.9725; IR (neat): $\tilde{\nu}$ = 3235, 1705, 1563, 1468, 1409, 1368, 1331, 1268, 1231, 1170, 1059, 915 cm^{-1}.

***N*-(3-(1*H*-Tetrazol-5-yl)phenyl)-4-bromo-2,6-difluorobenzenesulfonamide (13)**: White solid (325 mg, 78%); mp: 210–213 °C; ^1H NMR (400 MHz, CD$_3$OD): δ = 7.89 (td, *J* = 1.7, 0.8 Hz, 1H), 7.71 (ddd, *J* = 7.7, 1.7, 1.1 Hz, 1H), 7.46 (ddd, *J* = 8.2, 7.6, 0.5 Hz, 1H), 7.40–7.34 ppm (m, 3H); ^{13}C NMR (101 MHz, CD$_3$OD): δ = 159.40 (dd, $^1J_{C-F}$ = 261.6, $^3J_{C-F}$ = 5.0 Hz), 156.27, 137.90, 130.15, 127.83 (t, $^3J_{C-F}$ = 12.8 Hz), 125.63, 123.11, 122.41, 118.48, 116.82 (dd, $^2J_{C-F}$ = 26.9, $^4J_{C-F}$ = 3.9 Hz), 116.34 ppm (t, $^2J_{C-F}$ = 16.1 Hz); HRMS (ESI+): *m/z* $[M+MeCN+H]^+$ calcd for $C_{15}H_{12}BrF_2N_6O_2S$: 456.9894, found: 456.9904; IR (neat): $\tilde{\nu}$ = 3251, 3087, 2993, 2910, 2844, 2613, 2552, 2481, 1877, 1595, 1558, 1471, 1420, 1174, 1031, 918, 854 cm^{-1}.

***N*-(3-(1*H*-Tetrazol-5-yl)phenyl)-3,4-dimethylbenzenesulfonamide (14)**: White solid (273 mg, 83%); mp: 221–223 °C; ^1H NMR (400 MHz, CD$_3$OD): δ = 7.94 (m, 1H), 7.77 (m, 1H), 7.63 (m, 1H), 7.52 (m, 1H), 7.39 (m, 1H), 7.32 (m, 1H), 2.35 ppm (br s, 6H); ^{13}C NMR (101 MHz, CD$_3$OD): δ = 156.23, 142.61, 139.20, 137.81, 136.75, 129.99, 129.79, 127.62, 125.24, 124.55, 122.94, 122.51, 118.76, 18.52, 18.44 ppm; HRMS (ESI+): *m/z* $[M+MeCN+H]^+$ calcd for $C_{17}H_{19}N_6O_2S$: 371.1290, found: 371.1290; IR (neat): $\tilde{\nu}$ = 3246, 2360, 1576, 1481, 1326, 1151, 932 cm^{-1}.

***N*-(3-(1*H*-Tetrazol-5-yl)phenyl)-[1,1′-biphenyl]-4-sulfonamide (15)**: White solid (306 mg, 81%); mp: 206–210 °C; ^1H NMR (400 MHz, CD$_3$OD): δ = 8.03–7.99 (m, 3H), 7.86–7.79 (m, 3H), 7.72–7.68 (m, 2H), 7.58–7.51 (m, 3H), 7.49–7.44 ppm (m, 2H); ^{13}C NMR (101 MHz, CD$_3$OD): δ = 156.14, 145.81, 139.10, 139.06, 138.20, 130.11, 128.77, 128.23, 127.53, 127.30, 126.96, 125.47, 123.07, 122.75, 118.95 ppm; HRMS (ESI+): *m/z* $[M+MeCN+H]^+$ calcd for $C_{21}H_{19}N_6O_2S$: 419.1290, found: 419.1295; IR (neat): $\tilde{\nu}$ = 3239, 2857, 2717, 2466, 1588, 1480, 1400, 1368, 1325, 1157, 933, 680 cm^{-1}.

***N*-(3-(1*H*-Tetrazol-5-yl)phenyl)-7-chlorobenzo[*c*][1,2,5]oxadiazole-4-sulfonamide (16)**: Yellow solid (287 mg, 76%); mp: 168–170 °C; ^1H NMR (400 MHz, [D$_6$]acetone): δ = 8.20 (d, *J* = 7.4 Hz, 1H), 8.05 (td, *J* = 1.8, 0.8 Hz, 1H), 7.89–7.77 (m, 2H), 7.53–7.37 ppm (m, 2H); ^{13}C NMR (101 MHz, [D$_6$]acetone): δ = 157.46, 149.94, 146.03, 138.54, 136.80, 131.20, 131.06, 128.11, 127.87, 127.15, 124.32, 123.93, 119.86 ppm; HRMS (ESI+): *m/z* $[M+H]^+$ calcd for $C_{13}H_9ClN_7O_3S$: 378.0176, found: 378.0174; IR (neat): $\tilde{\nu}$ = 3289, 1692, 1597, 1493, 1427, 1346, 1275, 1228, 1153, 1040, 939 cm^{-1}.

***N*-(3-(1*H*-Tetrazol-5-yl)phenyl)benzo[*c*]thiophene-1-sulfonamide (17)**: White solid (261 mg, 73%); mp: 238–240 °C; ^1H NMR (400 MHz, [D$_6$]acetone): δ = 8.56 (s, 1H), 8.31 (ddd, *J* = 8.1, 1.4, 0.7 Hz, 1H), 8.06–7.99 (m, 2H), 7.78 (dt, *J* = 7.4, 1.5 Hz, 1H), 7.60–7.33 ppm (m, 4H); ^{13}C NMR (101 MHz, acetone): δ = 156.41, 140.34, 138.62, 136.37, 133.49, 132.87, 130.21, 126.09, 125.73, 125.58, 123.16, 123.00, 122.74, 122.24, 118.27 ppm; HRMS (ESI+): *m/z* $[M+MeCN+H]^+$ calcd for $C_{17}H_{15}N_6O_2S_2$: 399.0698, found: 399.0710; IR (neat): $\tilde{\nu}$ = 3422, 3096, 2814, 1569, 1481, 1150, 935, 744, 587 cm^{-1}.

***N*-(3-(1*H*-Tetrazol-5-yl)phenyl)benzo[*b*]thiophene-2-sulfonamide (18)**: White solid (243 mg, 68%); mp: 205–208 °C; ^1H NMR (400 MHz, CD$_3$OD): δ = 7.93 (ddd, *J* = 2.2, 1.7, 0.5 Hz, 1H), 7.89–7.83 (m, 3H), 7.72 (ddd, *J* = 7.7, 1.7, 1.1 Hz, 1H), 7.50–7.35 ppm (m, 3H); ^{13}C NMR (101 MHz, CD$_3$OD): δ = 156.26, 141.61, 140.09, 138.50, 137.48, 129.98, 129.63, 127.08, 125.49, 125.35, 125.17, 123.21, 123.07, 122.26, 119.17 ppm; HRMS (ESI+): *m/z* $[M+MeCN+H]^+$ calcd for $C_{17}H_{15}N_6O_2S_2$: 399.0698, found: 399.0698; IR (neat): $\tilde{\nu}$ = 3602, 3520, 3249, 2912, 2762, 2642, 2428, 1592, 1562, 1484, 1421, 1358, 1152, 873 cm^{-1}.

***N*-(3-(1*H*-Tetrazol-5-yl)phenyl)-1-methyl-1*H*-indole-6-sulfonamide (19)**: White solid (269 mg, 76%); mp: 235–240 °C; ^1H NMR (400 MHz, CD$_3$OD): δ = 8.21 (m, 1H), 7.95 (m, 1H), 7.74–7.70 (m, 2H), 7.52 (m, 1H), 7.46 (m, 1H), 7.39 (ddd, *J* = 8.2, 2.2, 1.1 Hz, 1H), 7.36 (d, *J* = 3.2 Hz, 1H), 6.63 (dd, *J* = 3.2, 0.9 Hz, 1H), 3.87 ppm (s, 3H); ^{13}C NMR (101 MHz, CD$_3$OD): δ = 156.22, 139.52, 138.57, 131.48, 129.87, 129.59, 127.81, 125.15, 122.86, 122.30, 121.08, 119.44, 118.74, 109.49, 102.02, 31.79 ppm; HRMS (ESI+): *m/z* $[M+H]^+$ calcd for $C_{16}H_{15}N_6O_2S$: 355.0977, found: 355.0981; IR (neat): $\tilde{\nu}$ = 3245, 3014, 2360, 1575, 1480, 1151, 1049, 934 cm^{-1}.

***N*-(3-(1*H*-Tetrazol-5-yl)phenyl)thiophene-2-sulfonamide (20)**: White solid (243 mg, 79%); mp: 175–180 °C; ^1H NMR (400 M, CD$_3$OD): δ = 7.99 (m, 1H), 7.87–7.78 (m, 2H), 7.67 (dd, *J* = 3.8, 1.4 Hz, 1H), 7.57 (m, 1H), 7.45 (ddd, *J* = 8.1, 2.2, 1.1 Hz, 1H), 7.15 ppm (dd, *J* = 5.0, 3.8 Hz, 1H); ^{13}C NMR (101 MHz, CD$_3$OD): δ = 156.23, 139.99, 138.83, 132.53, 132.51, 130.06, 127.08, 125.38, 123.38, 123.02, 119.20 ppm; HRMS (ESI+): *m/z* $[M+MeCN+H]^+$ calcd for $C_{13}H_{13}N_6O_2S_2$: 349.0541, found: 349.0538; IR (neat): $\tilde{\nu}$ = 3237, 2360, 1574, 1480, 1326, 1156, 1039, 931, 717 cm^{-1}.

***N*-(3-(1*H*-Tetrazol-5-yl)phenyl)benzenesulfonamide (21)**: White solid (214 mg, 71%); mp: 179–183 °C; ^1H NMR (400 MHz, CD$_3$OD): δ = 7.99–7.88 (m, 3H), 7.78 (ddd, *J* = 7.7, 1.7, 1.0 Hz, 1H), 7.65 (m, 1H), 7.61–7.54 (m, 2H), 7.51 (ddd, *J* = 8.2, 7.7, 0.5 Hz, 1H), 7.39 ppm (ddd, *J* = 8.2, 2.2, 1.0 Hz, 1H); ^{13}C NMR (101 MHz, CD$_3$OD): δ = 156.24, 139.55, 139.00, 132.79, 130.04, 128.86, 126.88, 125.31, 123.15, 122.72, 118.97 ppm; HRMS (ESI+): *m/z* $[M+MeCN+H]^+$ calcd for $C_{15}H_{15}N_6O_2S$ 343.0977, found: 343.0974; IR (neat): $\tilde{\nu}$ = 3239, 2898, 2360, 1576, 1481, 1233, 1161, 1089, 1040, 932, 683 cm^{-1}.

***N*-(3-(1*H*-Tetrazol-5-yl)phenyl)pyridine-3-sulfonamide (22)**: White solid (154 mg, 51%); mp: 219–223 °C; ^1H NMR (400 MHz, CD$_3$OD): δ = 8.92 (m, 1H), 8.70 (m, 1H), 8.19 (m, 1H), 7.86 (m, 1H), 7.74 (m, 1H), 7.54 (m,1H), 7.46 (ddd, *J* = 8.2, 7.7, 0.5 Hz, 1H), 7.31 ppm (m, 1H); ^{13}C NMR (101 MHz, CD$_3$OD): δ = 156.31, 152.83, 147.12, 138.22, 136.46, 135.24, 130.16, 125.73, 124.11, 123.32, 123.19, 119.19 ppm; HRMS (ESI+): *m/z* $[M+H]^+$ calcd for $C_{12}H_{11}N_6O_2S$: 303.0664, found: 303.0670; IR (neat): $\tilde{\nu}$ = 2896, 2746, 2360, 1581, 1470, 1358, 1166, 1112 cm^{-1}.

4-Bromo-5-chloro-*N*-(3-cyanophenyl)-*N*-methylthiophene-2-sulfonamide (24): To a solution of 3-aminobenzonitrile (**23**) (1.0 mmol) in anhydrous CH_2Cl_2 (5 mL), under an atmosphere of nitrogen, was added 4-bromo-5-chlorothiophene-2-sulfonyl chloride (1.2 mmol) and pyridine (3.0 mmol). The resulting reaction mixture was stirred at RT overnight and then quenched with saturated aq NH_4Cl (20 mL). The aqueous phase was extracted with CH_2Cl_2 (3×10 mL). The combined organic phase was dried over Na_2SO_4, filtered and evaporated under reduced pressure. The crude product (91% purity determined by LCMS) obtained was dissolved in dry tetrahy-

drofuran (THF) and cooled to 0 °C. NaH (60% dispersion in mineral oil) (1.2 mmol) was added under nitrogen atmosphere. The solution was stirred for 30 min. CH_3I (1.5 mmol) was then added dropwise, and the solution was stirred at 25 °C for 3 h. The reaction mixture was quenched with saturated aq NH_4Cl (20 mL), and the aqueous phase was extracted with CH_2Cl_2 (3×10 mL). The combined organic phase was dried over Na_2SO_4, filtered and evaporated under reduced pressure to afford crude product, which was purified by silica gel flash column chromatography (isohexane/EtOAc, 90:10→80:20) to give product **24** as a white solid (306 mg, 78%); mp: 138–140 °C; ^{1}H NMR (400 MHz, [D$_6$]DMSO): δ = 7.84 (dd, J = 6.0, 1.9 Hz, 2H), 7.71 (d, J = 0.8 Hz, 1H), 7.69–7.58 (m, 2H), 3.26 ppm (s, 3H); ^{13}C NMR (101 MHz, [D$_6$]DMSO): δ = 141.48, 135.29, 133.89, 133.59, 132.38, 132.12, 130.93, 130.50, 118.40, 112.84, 112.53, 38.19 ppm; HRMS (ESI+): m/z $[M+H]^+$ calcd for $C_{12}H_9BrClN_2O_2S_2$: 390.8977, found: 390.8976; IR (neat): $\tilde{\nu}$ = 3088, 3070, 2223, 1603, 1580, 1482, 1455, 1436, 1401, 1355, 1311, 1270, 1196, 1158, 1140, 1070, 1018, 933 cm^{-1}.

***N*-(3-(1*H*-Tetrazol-5-yl)phenyl)-4-bromo-5-chloro-*N*-methylthiophene-2-sulfonamide (25)**: The mixture of nitrile **24** (1.0 mmol), NaN_3 (2.0 mmol), and Et_3N·HCl (2.0 mmol) in dry toluene (5 mL) was heated at reflux for 12 h with constant stirring. After cooling, the reaction mixture was acidified (pH 2) using 2 N aq HCl and extracted with CH_2Cl_2 (3×20 mL). The combined organic phase was dried over Na_2SO_4, filtered and evaporated under reduced pressure to afford the crude product, which was purified by silica gel flash column chromatography (CH_2Cl_2/MeOH, 95:05→90:10) to give product **25** as a white solid (309 mg, 71%); mp: 152–154 °C; ^{1}H NMR (400 MHz, [D$_6$]acetone): δ = 8.14 (ddd, J = 7.8, 1.7, 1.1 Hz, 1H), 8.06 (ddd, J = 2.2, 1.7, 0.5 Hz, 1H), 7.65 (ddd, J = 8.2, 7.8, 0.5 Hz, 1H), 7.53 (ddd, J = 8.1, 2.3, 1.1 Hz, 1H), 7.49 (s, 1H), 3.42 ppm (s, 3H); ^{13}C NMR (101 MHz, [D$_6$]acetone): δ = 156.40, 141.79, 134.76, 134.29, 133.34, 130.22, 129.01, 126.37, 126.20, 125.32, 111.72, 37.79 ppm; HRMS (ESI+): m/z $[M+H]^+$ calcd for $C_{12}H_{10}BrClN_5O_2S_2$: 433.9148, found: 433.9145; IR (neat): $\tilde{\nu}$ = 1712, 1558, 1454, 1398, 1354, 1154, 1067, 1018, 909 cm^{-1}.

***N*-(3-(1*H*-Tetrazol-5-yl)phenyl)-4-bromo-5-chlorothiophene-2-carboxamide (27)**: 4-Bromo-5-chlorothiophene-2-carboxylic acid (**26**) (1.0 mmol) was dissolved in dry DMF, and PyBOP (1.5 mmol) was added. The solution was stirred at 25 °C for 30 min. 3-(1*H*-Tetrazol-5-yl)aniline (**4**) (2.0 mmol) and Et_3N (2.0 mmol) were then added, and the stirring continued for an additional 18 h. The reaction mixture was then diluted with water (10 mL) and extracted with EtOAc (3×10 mL). The combined organic phase was dried over Na_2SO_4, filtered and evaporated under reduced pressure to afford the crude product, which was purified by silica gel flash column chromatography (CH_2Cl_2/MeOH, 97:03→90:10) to give product **27** as a white solid (312 mg, 81%); mp: 263–265 °C; ^{1}H NMR (400 MHz, [D$_6$]DMSO): δ = 10.61 (s, 1H), 8.49 (t, J = 1.9 Hz, 1H), 8.15 (d, J = 0.6 Hz, 1H), 7.91 (ddd, J = 8.2, 2.2, 1.0 Hz, 1H), 7.77 (ddd, J = 7.7, 1.7, 1.0 Hz, 1H), 7.60 ppm (t, J = 8.0 Hz, 1H); ^{13}C NMR (101 MHz, [D$_6$]DMSO): δ = 158.12, 155.68, 139.09, 138.06, 131.52, 131.05, 130.02, 124.94, 122.55, 122.49, 118.47, 110.96 ppm; HRMS (ESI+): m/z $[M+H]^+$ calcd for $C_{12}H_8BrClN_5OS$: 383.9321, found: 383.9319; IR (neat): $\tilde{\nu}$ = 3284, 2883, 1739, 1631, 1591, 1539, 1407, 1303, 1178, 1079, 1028 cm^{-1}.

Biology

The enzymatic assay applied for screening purposes as well as follow-up dose–response characterization was based on the use of membrane preparations from CHO cells as a source of enzymatic activity. These cells are known to abundantly express IRAP and contain minimal amounts of contaminating APN activities.[36] The CHO cell membrane preparation was conducted based on the procedure described by Demaegt et al.[37] with lysis of washed cells being done by means of ultrasonication followed by multiple strokes (>20) with a Dounze homogenizer and a centrifugation (30000×g for 30 min at 4 °C) procedure for pelleting and washing of the membranes.

The extent of enzymatic activity in each sample was quantified in a microtiter-based screening assay using the peptide-like substrate L-leucine-*p*-nitroanilide (L-Leu-*p*NA; Sigma–Aldrich, product no. L9125), which upon IRAP-mediated cleavage produces *para*-nitroaniline that absorbs at 405 nm.[37] The screening campaign was performed at Chemical Biology Consortium Sweden (CBCS) using a primary screening set of 10500 compounds[38] (majority of compounds donated by Biovitrum AB, Stockholm, Sweden). The screen was conducted in a 384-well format, whereas follow-up dose–response experiments were conducted in a transparent 96-well plate (Nunc, product no. 269620).

In this format, the final assay volume was 200 μL in an assay buffer consisting of 50 mM Tris-HCl, 150 mM NaCl, and 0.1 mM phenylmethanesulfonylfluoride (PMSF) at pH 7.4. The assays were conducted in the presence of a final concentration of 1 mM L-Leu-*p*NA and homogenized CHO cell membranes from 50000–200000 cells per well, depending on test occasion and membrane batch. The protocol for running the dose–response assay started with a serial dilution of the compound stock solutions at 10 mM in 99.9 % anhydrous DMSO (Sigma–Aldrich) by a factor of 1/3 in columns 1–11 of the 96-well plates. Column 12 was reserved for controls: the equivalent amount of DMSO was added to wells A12–D12 (negative controls representing 0% inhibition of the enzyme), whereas a 10 mM stock solution of **3** was placed in wells E12–H12 serving as controls representing 100% inhibition of the enzyme activity. The DMSO solutions were then diluted in assay buffer and transferred to the transparent assay plates in triplicate (50 μL to each well both for samples and controls), followed by addition of diluted homogenized CHO cell membranes (50 μL) and substrate (100 μL) to initiate the enzymatic reaction. The plates were covered and then incubated at RT until a statistically significant difference was observed (6–12 h) between the controls ($Z' > 0.8$). Care was taken to ensure the readings were taken at a time point when the absorbance signal still increased linearly with time. Raw data were then imported into Microsoft Excel for conversion to % inhibition data based on the controls on each plate. After data from triplicate samples were averaged, the curves were fitted to a four-parameter dose–response model within XLfit (model 205) to obtain best-fit values for the IC_{50}, Hill slope, and the upper and lower limits of the dose–response curve.

Computational methods

Docking was conducted using Glide (version 5.8, Schrödinger, LLC, New York, NY, 2012) SP mode.[39–41] The crystal structure 4FYT was downloaded from the Protein Data Bank (PDB)[42] and prepared using the Protein Preparation Wizard (Schrödinger Suite 2012 Protein Preparation Wizard; Epik version 2.2, Schrödinger, LLC, New York, NY, 2012; Impact version 5.7, Schrödinger, LLC, New York, NY, 2012; Prime version 2.3, Schrödinger, LLC, New York, NY, 2012) in Maestro (version 9.3, Schrödinger, LLC, New York, NY, 2012). All water molecules were deleted, hydrogen bond assignments were optimized, and a minimization of the hydrogens was carried out. The structures were prepared for docking using LigPrep (version

2.5, Schrödinger, LLC, New York, NY, 2012) generating different protonation states.

Acknowledgements

Funding for the work carried out at Chemical Biology Consortium Sweden (CBCS) was provided by the Swedish Research Council and Karolinska Institutet, Sweden (A.J.J., H.A., K.S,. and T.L). The Karolinska High Throughput Center (KHTC) led by Prof. Jussi Taipale is acknowledged for kindly providing access to an automated screening line. Grants from the Swedish Research Council and the Kjell and Märta Beijer Foundation to the Department of Pharmaceutical Biosciences and to the Department of Medicinal Chemistry at Uppsala University are acknowledged.

Keywords: aminopeptidases · arylsulfonamides · insulin-regulated aminopeptidase (IRAP) · structure–activity relationships · cognitive enhancers

[1] J. J. Braszko, G. Kupryszewski, B. Witczuk, K. Wisniewski, *Neuroscience* **1988**, *27*, 777 – 83.
[2] J. J. Braszko, P. Wielgat, A. Walesiuk, *Neuropeptides* **2008**, *42*, 301 – 309.
[3] D. De Bundel, I. Smolders, R. Yang, A. L. Albiston, Y. Michotte, S. Y. Chai, *Neurobiol. Learn. Mem.* **2009**, *92*, 19 – 26.
[4] P. R. Gard, C. Naylor, S. Ali, C. Partington, *Eur. J. Pharmacol.* **2012**, *683*, 155 – 160.
[5] J. W. Wright, L. Stubley, E. S. Pederson, E. A. Kramár, J. M. Hanesworth, J. W. Harding, *J. Neurosci.* **1999**, *19*, 3952 – 3961.
[6] J. Lee, T. Mustafa, S. G. McDowall, F. A. Mendelsohn, M. Brennan, R. A. Lew, A. L. Albiston, S. Y. Chai, *J. Pharmacol. Exp. Ther.* **2003**, *305*, 205 – 211.
[7] A. L. Albiston, S. Diwakarla, R. N. Fernando, S. J. Mountford, H. R. Yeatman, B. Morgan, V. Pham, J. K. Holien, M. W. Parker, P. E. Thompson, S. Y. Chai, *Br. J. Pharmacol.* **2011**, *164*, 37 – 47.
[8] S. Y. Chai, H. R. Yeatman, M. W. Parker, D. B. Ascher, P. E. Thompson, H. T. Mulvey, A. L. Albiston, *BMC Neurosci.* **2008**, *9*, S14.
[9] J. W. Harding, V. I. Cook, A. V. Miller-Wing, J. M. Hanesworth, M. F. Sardinia, K. L. Hall, J. W. Stobb, G. N. Swanson, J. K. Coleman, J. W. Wright, E. C. Harding, *Brain Res.* **1992**, *583*, 340 – 343.
[10] G. N. Swanson, J. M. Hanesworth, M. F. Sardinia, J. K. Coleman, J. W. Wright, K. L. Hall, A. V. Miller-Wing, J. W. Stobb, V. I. Cook, E. C. Harding, J. W. Harding, *Regul. Pept.* **1992**, *40*, 409 – 419.
[11] A. L. Albiston, S. G. McDowall, D. Matsacos, P. Sim, E. Clune, T. Mustafa, J. Lee, F. A. Mendelsohn, R. J. Simpson, L. M. Connolly, S. Y. Chai, *J. Biol. Chem.* **2001**, *276*, 48623 – 48626.
[12] T. Rogi, M. Tsujimoto, H. Nakazato, S. Mizutani, Y. Tomoda, *J. Biol. Chem.* **1996**, *271*, 56 – 61.
[13] M. Tsujimoto, S. Mizutani, H. Adachi, M. Kimura, H. Nakazato, Y. Tomoda, *Arch. Biochem. Biophys.* **1992**, *292*, 388 – 392.
[14] T. E. Rasmussen, S. Pedraza-Diaz, R. Hardre, P. G. Laustsen, A. G. Carrion, T. Kristensen, *Eur. J. Biochem.* **2000**, *267*, 2297 – 2306.
[15] R. A. Lew, T. Mustafa, S. Ye, S. G. McDowall, S. Y. Chai, A. L. Albiston, *J. Neurochem.* **2003**, *86*, 344 – 350.
[16] J. W. Wright, J. W. Harding, *J. Renin Angiotensin Aldosterone Syst.* **2008**, *9*, 226 – 237.
[17] H. Andersson, M. Hallberg, *Int. J. Hypertens.* **2012**, *2012*, 1.
[18] P. R. Gard, *BMC Neurosci.* **2008**, *9*, S15.
[19] B. Stragier, D. De Bundel, S. Sarre, I. Smolders, G. Vauquelin, A. Dupont, Y. Michotte, P. Vanderheyden, *Heart Failure Rev.* **2008**, *13*, 321 – 337.
[20] L. H. Kawas, A. T. McCoy, B. J. Yamamoto, J. W. Wright, J. W. Harding, *J. Pharmacol. Exp. Ther.* **2012**, *340*, 539 – 548.
[21] P. M. Vanderheyden, *Mol. Cell. Endocrinol.* **2009**, *302*, 159 – 66.
[22] H. Andersson, H. Demaegdt, A. Johnsson, G. Vauquelin, G. Lindeberg, M. Hallberg, M. Erdelyi, A. Karlen, A. Hallberg, *J. Med. Chem.* **2011**, *54*, 3779 – 3792.
[23] H. Andersson, H. Demaegdt, G. Vauquelin, G. Lindeberg, A. Karlen, M. Hallberg, *Bioorg. Med. Chem.* **2008**, *16*, 6924 – 6935.
[24] H. Andersson, H. Demaegdt, G. Vauquelin, G. Lindeberg, A. Karlen, M. Hallberg, M. Erdelyi, A. Hallberg, *J. Med. Chem.* **2010**, *53*, 8059 – 8071.
[25] S. J. Mountford, A. L. Albiston, W. N. Charman, L. Ng, J. K. Holien, M. W. Parker, J. A. Nicolazzo, P. E. Thompson, S. Y. Chai, *J. Med. Chem.* **2014**, *57*, 1368 – 1377.
[26] A. L. Albiston, C. J. Morton, H. L. Ng, V. Pham, H. R. Yeatman, S. Ye, R. N. Fernando, D. De Bundel, D. B. Ascher, F. A. Mendelsohn, M. W. Parker, S. Y. Chai, *FASEB J.* **2008**, *22*, 4209 – 4217.
[27] S. Byström, K. Färnegårdh, C. Hedgecock, E. Homan, M. Jönsson, T. Lundbäck, J. Martinsson, M. Sari, (KANCERA AB, Solna, Sweden), Int. PCT Pub. No. WO/2012/035171 A3, **2012**.
[28] K. Koguro, T. Oga, S. Mitsui, R. Orita, *Synthesis* **1998**, 910 – 914.
[29] J. Coste, D. Lenguyen, B. Castro, *Tetrahedron Lett.* **1990**, *31*, 205 – 208.
[30] A. H. Wong, D. Zhou, J. M. Rini, *J. Biol. Chem.* **2012**, *287*, 36804 – 36813.
[31] A. L. Albiston, V. Pham, S. Ye, L. Ng, R. A. Lew, P. E. Thompson, J. K. Holien, C. J. Morton, M. W. Parker, S. Y. Chai, *Mol. Pharmacol.* **2010**, *78*, 600 – 607.
[32] A. Papakyriakou, E. Zervoudi, E. A. Theodorakis, L. Saveanu, E. Stratikos, D. Vourloumis, *Bioorg. Med. Chem. Lett.* **2013**, *23*, 4832 – 4836.
[33] C. J. Carrell, H. L. Carrell, J. Erlebacher, J. P. Glusker, *J. Am. Chem. Soc.* **1988**, *110*, 8651 – 8656.
[34] J. Birks, *Cochrane Database Syst. Rev.* **2006**, *1*, CD005593.
[35] P. Raina, P. Santaguida, A. Ismaila, C. Patterson, D. Cowan, M. Levine, L. Booker, M. Oremus, *Ann. Intern. Med.* **2008**, *148*, 379 – 397.
[36] H. Demaegdt, P. J. Lenaerts, J. Swales, J. P. De Backer, H. Laeremans, M. T. Le, K. Kersemans, L. K. Vogel, Y. Michotte, P. Vanderheyden, G. Vauquelin, *Eur. J. Pharmacol.* **2006**, *546*, 19 – 27.
[37] H. Demaegdt, P. Vanderheyden, J. P. De Backer, S. Mosselmans, H. Laeremans, M. T. Le, V. Kersemans, Y. Michotte, G. Vauquelin, *Biochem. Pharmacol.* **2004**, *68*, 885 – 892.
[38] These compounds are stored at room temperature under nitrogen atmosphere as 10 mM solutions in DMSO in Labcyte 384 LDV source plates, from which they are dispensed using a Labcyte Echo acoustic dispenser.
[39] R. A. Friesner, J. L. Banks, R. B. Murphy, T. A. Halgren, J. J. Klicic, D. T. Mainz, M. P. Repasky, E. H. Knoll, M. Shelley, J. K. Perry, D. E. Shaw, P. Francis, P. S. Shenkin, *J. Med. Chem.* **2004**, *47*, 1739 – 1749.
[40] R. A. Friesner, R. B. Murphy, M. P. Repasky, L. L. Frye, J. R. Greenwood, T. A. Halgren, P. C. Sanschagrin, D. T. Mainz, *J. Med. Chem.* **2006**, *49*, 6177 – 6196.
[41] T. A. Halgren, R. B. Murphy, R. A. Friesner, H. S. Beard, L. L. Frye, W. T. Pollard, J. L. Banks, *J. Med. Chem.* **2004**, *47*, 1750 – 1759.
[42] F. C. Bernstein, T. F. Koetzle, G. J. Williams, E. F. Meyer Jr., M. D. Brice, J. R. Rodgers, O. Kennard, T. Shimanouchi, M. Tasumi, *J. Mol. Biol.* **1977**, *112*, 535 – 542.

Received: August 12, 2014
Published online on November 21, 2014